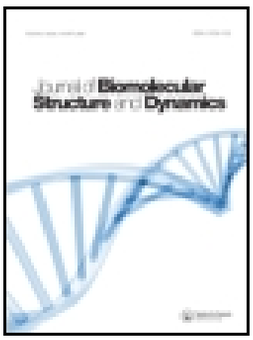

Taylor & Francis
Taylor & Francis Group

Journal of Biomolecular Structure and Dynamics

ISSN: (Print) (Online) Journal homepage: https://www.tandfonline.com/loi/tbsd20

New imino-methoxy derivatives: design, synthesis, characterization, antimicrobial activity, DNA interaction and molecular docking studies

Sultan Onur, Mustafa Çeşme, Muhammet Köse & Ferhan Tümer

To cite this article: Sultan Onur, Mustafa Çeşme, Muhammet Köse & Ferhan Tümer (2021): New imino-methoxy derivatives: design, synthesis, characterization, antimicrobial activity, DNA interaction and molecular docking studies, Journal of Biomolecular Structure and Dynamics, DOI: 10.1080/07391102.2021.1955741

To link to this article: https://doi.org/10.1080/07391102.2021.1955741

JOURNAL OF BIOMOLECULAR STRUCTURE AND DYNAMICS
https://doi.org/10.1080/07391102.2021.1955741

Taylor & Francis
Taylor & Francis Group

New imino-methoxy derivatives: design, synthesis, characterization, antimicrobial activity, DNA interaction and molecular docking studies

Sultan Onur, Mustafa Çeşme, Muhammet Köse and Ferhan Tümer

Department of Chemistry, Faculty of Art and Sciences, Kahramanmaraş Sütçü İmam University, Kahramanmaraş, Turkey

Communicated by Ramaswamy H. Sarma

ABSTRACT

Four new diarylmethylamine imine compounds (5a-5d) were prepared in order to examine their DNA binding properties, antimicrobial activity and molecular docking. The compounds were characterized by the common spectroscopic and analytic methods. Furthermore, solid-state structure of compounds 5a and 5c were determined by single-crystal X-ray diffraction studies. The compounds were then investigated for their DNA binding properties employing UV absorption, fluorescence spectroscopy under the physiological pH condition Tris-HCl buffer at pH 7.4. The compounds 5a-5d showed moderate binding constants with Kb values of $3.56 \pm 0.3 \times 10^4$, $2.18 \pm 0.2 \times 10^5$, $1.44 \pm 0.3 \times 10^5$ and $2.56 \pm 0.3 \times 10^4$ M^{-1}, respectively. The molecular dockings were performed to investigate the ligand-DNA interactions. The in-silico DNA-compound interaction studies showed that the compounds interact with DNA in groove binding mode. Antimicrobial activity studies of imine compounds were tested against *E. coli* as bacteria, *S. typhimurium*, *S. aureus*, *B. cereus*, *B. subtilis*, and *C. albicans* as fungi. While all compounds show moderate activity against bacteria, no activity against fungi has been investigated.

ARTICLE HISTORY
Received 26 March 2021
Accepted 10 July 2021

KEYWORDS
Imino-methoxy; diarylmethylamine; X-ray structure; DNA binding; molecular docking

1. Introduction

Diarylmethylamine derivatives are molecules that attract attention in organic chemistry due to their pharmaceutical and distinctive chemical properties. Diarylmethylamine units are commonly found in a variety of biologically active compounds such as anticancer, anti-tuberculosis, antimalarial, antiviral, potent and selective non-steroidal aromatase inhibitors (NSAIs) and anti-HCV (Hepatitis C Virus) agents (Ameen & Snape, 2013; Ashton et al., 1984; Cardellicchio et al., 2010; Di Santo et al., 2005; Gemma et al., 2007; Plobeck et al., 2000; Roy & Panda, 2020; Thomas et al., 2001). Imine compounds constitute the class of compounds that are intensively researched due to their photochromic and thermochromic properties, tautomeric balance, analytical applications, as well as their biological and pharmacological properties. Due to the convenience of the synthesis stage and the ability of the ligands to flex easily, the fact that they are suitable ligands for the determination and coordination of many metal ions has caused these compounds to gain significant importance (Soliman & Linert, 2007). Since carbon and nitrogen (C = N) in Schiff bases prevent double bond rotation, the orientation of the connected groups creates isomeric structures. Since the C = N bond is freer than the C = C bond, it is possible for the stereoisomers to transform into one another (Allan et al., 1992). Schiff bases (Ph-CH = N-Ph, Ph-CH = N-R) containing only imine groups as functional groups are the best Schiff bases that contain groups such as -OH, $-NH_2$, -SH, $-OCH_3$ in *ortho*-position (Göppert-Mayer, 1931).

The fact that the complexes formed by the ligands containing atoms such as oxygen, nitrogen and sulfur in their structures display different activities (antitumor, antiviral, antifungal, antibacterial) and being used in the industrial field increased the interest in this field (Lakshmi et al., 2012; McCord & Fridovich, 1969; Riley et al., 1997). When Schiff, some metal complexes are used as a binding agent or reactive monomer, the metal-containing polymers have been synthesized and used in numerous applications with this polymer (Yang et al., 2013).

Deoxyribonucleic acid (DNA) is one of the biopolymers that contain genetic instructions used in the development and functioning of all known living organisms and are also essential for all known life forms (Dahm, 2005). DNA has two primary functions; transcription and replication. The transcription process of DNA refers to the conversion of genetic information from DNA to RNA to synthesize proteins in the body, including hormones, enzymes, and receptors. In other words, it is the transfer of genetic information from DNA to RNA. On the other hand, DNA replication is a biological process that occurs in all organisms and forms the basis of heredity by copying DNA (J. H. Shi et al., 2015a). Transcription and replication are essential for cell survival, proliferation and the systematic functioning of all physiological processes. Medicinal chemists mainly focus on DNA interactions with drugs or ligands (novel compounds and drug candidates), commonly called small molecules. Generally, small molecules bind to DNA through three dominant non-covalent modes

CONTACT Ferhan Tümer ftumer@ksu.edu.tr Department of Chemistry, Faculty of Art and Sciences, Kahramanmaraş Sütçü İmam University, Kahramanmaraş, Turkey.

Supplemental data for this article can be accessed online at https://doi.org/10.1080/07391102.2021.1955741.

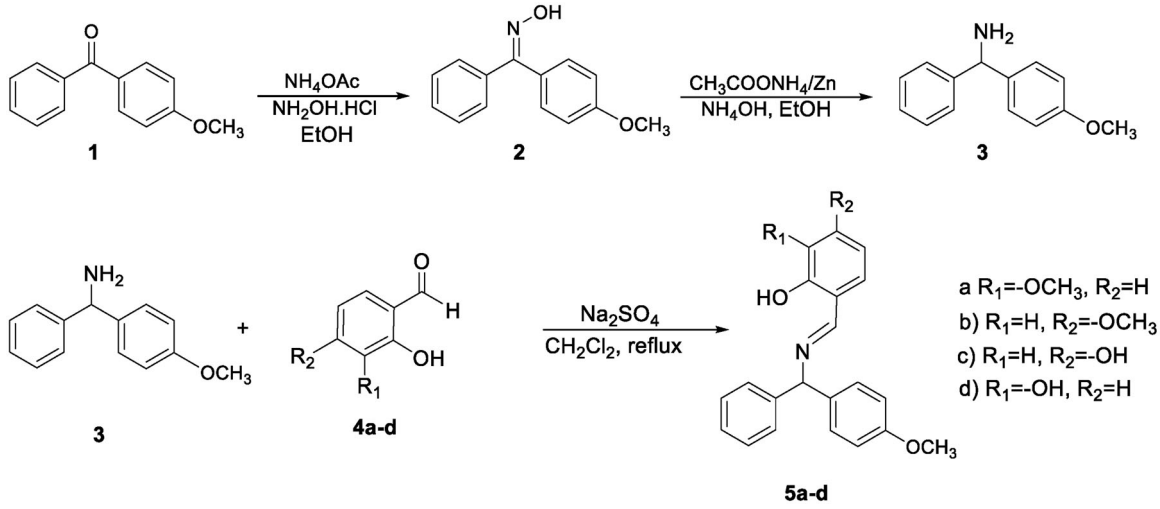

Scheme 1. General synthesis procedure of compounds.

called intercalative binding, groove binding, and electrostatic interactions (Adı mcı lar et al., 2021; Güngör et al., 2019). Consequently, synthetic or natural small molecules or currently commercially available drug compounds can be used as drugs to inhibit or activate DNA function to ameliorate or manage the disease. For this reason, the examination of the intermolecular relationship between small molecules/drugs and DNA using spectroscopic and theoretical methods has increasingly become an area of interest for many researchers (Dong et al., 2018; J.-H. H. Shi et al., 2018; J. H. Shi et al., 2018; J. H. Shi et al., 2015a; Wang et al., 2020).

In our previous work, we reported the synthesis and antibacterial properties of a series of diarylmethylamine imine compounds (Onur et al., 2020). In continuation of our interest in the synthesis and biological properties of these compounds, four new imine compounds with hydroxyl and methoxy substitute groups (Scheme 1) were prepared and their DNA binding properties were investigated. In addition, biological and molecular docking studies have evaluated the suitability of these derivatives for applications in biological systems.

DNA binding of newly synthesized compounds was investigated using fluorescence quenching and UV-Vis spectroscopy. The atomic details of these ligand-DNA interactions were investigated by the molecular placement method. Results based on in silico dna-ligand interaction studies show that all ligands are corrugated binders, and that H-bond interactions play a fundamental role in the stability of these ligand-DNA complexes. This study demonstrates the mode of binding interaction, binding affinity, the main forces of interaction of ligands with FS-DNA, and details of the structure of the ligand-FS-DNA complex. The interaction of FS-DNA with ligands is important in pharmaceutical drug discovery. Based on molecular docking studies in silico, the binding score of DNA interaction of compounds is highly satisfactory.

2. Experimental

2.1. Materials and measurements

All chemicals and solvents were of reagent-grade quality and obtained from commercial suppliers (Sigma Aldrich or Merck) and have been used as received except otherwise noted. Fish sperm DNA (74782), Tris-HCl (RES3098T-B7), Ethidium bromide (EtBr) and Sodium chloride (≥99.5%) were supplied from Sigma Aldrich, USA. Elemental analyses (C, H, N) were performed using a Costech ECS 4010 (CHN). The NMR spectra data (^{1}H and ^{13}C NMR) were recorded on a Bruker Avance III HD 400 MHz Spectrometer and TMS was used as an internal standard. Absorption measurements were performed using a double-beam spectrophotometer (Perkin Elmer, Lambda 45, USA) equipped with 1.0 cm quartz cells. Fluorescence spectra were collected on a Perkin Elmer LS55 photoluminescence spectrophotometer analyzer. Infrared spectra were recorded on a Perkin-Elmer FT-IR spectrometer (Spectrum 400) kitted with an ATR apparatus. Thermo Scientific Orion Star A215 was utilized for the measurement of pH values.

2.2. Synthesis of the compounds

2.2.1. General procedure for the preparation of oxime 2 and diarylmethylamine 3

The synthesis of oxime **2** and diarylmethylamine **3** was carried out using a literature method (Onur et al., 2020).

2.2.2. General method for the synthesis of imine compounds (5a-d)

Compound 5a-5d was obtained according to our previous report (Onur et al., 2020). To a stirring solution of (4-methoxyphenyl)(phenyl)methanamine (4 g; 20.27 mmol) CH_2Cl_2 (40 mL) under nitrogen atmosphere, potassium carbonate (4 g; 29 mmol) was added followed by addition of salicylaldehyde derivatives (20.27 mmol). After stirring for 10–15 min, sodium sulfate (4 g; 28 mmol) were added and resulting mixture were stirred at room temperature for 24 h. The progress of the reaction was followed by TLC. The mixture was filtered. After removing the solvent, the oily residue was obtained and this was filtered over silica gel using ethyl acetate/hexane (1: 9) as eluent. Solvent was removed on a rotary evaporator and resulting solid was re-crystallized from ethanol.

5a: Yield 4.6 g (71%), color: yellow. melting point: 123–125 °C. FTIR: ($\nu_{max,}$ cm^{-1}): 3443, 3049, 2833, 1620, 1503,

1460, 1246, 1174, 1078, 1037, 971, 822, 751 cm^{-1}. ^1H NMR (400 MHz, $CDCl_3$, δ ppm): 1H NMR (400 MHz, $CDCl_3$) δ 14.21 (s, 1H), 8.47 (s, 1H), 7.34 (m, 7H), 6.90 (m, 5H), 5.62 (s, 1H), 3.94 (s, 3H), 3.80 (s, 3H). ^{13}C NMR (101 MHz, CDCl3) δ 164.77, 158.90, 151.59, 148.47, 142.81, 134.77, 128.70, 128.58, 127.35, 127.31, 123.19, 118.73, 118.21, 114.22, 114.10, 77.44, 77.12, 76.81, 75.82, 56.12, 55.30. Anal. Calcd for $C_{22}H_{21}NO_3$: C, 76.06; H, 6.09; N, 4.03. Found C, 76.15; H, 5.98; N, 4.10.

5b: Yield 3.65 g (58%), color: light yellow. melting point:114–116 °C. FTIR: ($\nu_{max,}$ cm^{-1}): 3431, 3006, 2958, 2839, 1621, 1510, 1443, 1386, 1292, 1166, 1033, 960, 833, 732 cm^{-1}. 1H NMR (400 MHz, $CDCl_3$) δ 14.10 (s, 1H), 8.36 (s, 1H), 7.40 − 7.34 (m, 4H), 7.30 − 7.24 (m, 3H), 7.16 (d, $J = 8.4$ Hz, 1H), 6.91 (d, $J = 7.0$ Hz, 1H), 6.51 (d, $J = 2.0$ Hz, 1H), 6.45 (dd, $J = 8.5$, 2.3 Hz, 1H), 5.59 (s, 1H), 3.84 (s, 3H), 3.81 (s, 3H). ^{13}C NMR (101 MHz, CDCl3) δ 164.22, 163.84, 163.58, 158.88, 142.98, 134.92, 132.90, 128.68, 128.65, 127.42, 127.28, 114.08, 112.68, 106.51, 101.17, 77.39, 77.08, 76.76, 75.35, 55.40, 55.30. Anal.Calcd for $C_{22}H_{21}NO_3$: C, 76.06; H, 6.09; N, 4.03. Found C, 76.45; H, 5.72; N, 4.08.

5c: Yield 4.24 g (66%), color: orange. melting point:112–114 °C. FTIR: ($\nu_{max,}$ cm^{-1}): 3385, 3272, 3016, 2836, 1629, 1607, 1510, 1462, 1386, 1307, 1235, 1204, 1178, 1030, 866, 818, 740 cm^{-1}. ^1H NMR (400 MHz, $CDCl_3$) δ 8.38 (s, 1H), 7.41 − 7.34 (m, 5H), 7.27 (d, $J = 8.5$ Hz, 2H), 7.02 (dd, $J = 7.7$, 1.6 Hz, 1H), 6.93 (d, $J = 8.8$ Hz, 2H), 6.83 (dd, $J = 7.9$, 1.6 Hz, 1H), 6.75 (t, $J = 7.8$ Hz, 1H), 5.70 (s, 1H), 3.83 (s, 3H). ^{13}C NMR (101 MHz, $CDCl_3$) δ 164.58, 159.10, 151.84, 145.63, 142.06, 133.92, 128.82, 128.75, 127.60, 127.41, 122.38, 118.08, 117.43, 116.90, 114.24, 77.40, 77.28, 77.08, 76.76, 74.42, 55.33. Anal.Calcd for $C_{21}H_{19}NO_3$: C, 75.66; H, 5.74; N, 4.20. Found C, 76.30; H, 5.20; N, 4.23.

5d: Yield 3.98 g (62%), color: orange. melting point:128–130 °C, FTIR: ($\nu_{max,}$ cm^{-1}): 3401, 3024, 2903, 1627, 1578, 1462, 1364, 1253, 1220, 1169, 1118, 1021, 970, 890, 834, 750. 697 cm^{-1}. ^1H NMR (400 MHz, $CDCl_3$, δ ppm) δ 8.02 (s, 1H), 7.39 − 7.25 (m, 5H), 7.23 (d, $J = 8.7$ Hz, 2H), 6.92 (d, $J = 8.6$ Hz, 1H), 6.88 (d, $J = 8.5$ Hz, 2H), 6.43 (d, $J = 2.1$ Hz, 1H), 6.29 (dd, $J = 8.6$, 1.8 Hz, 1H), 5.62 (s, 1H), 3.78 (s, 3H). ^{13}C NMR (100 MHz, $CDCl_3$, δ ppm): 169.08, 163.32, 163.15, 159.07, 141.71, 134.26, 133.55, 128.83, 128.73, 127.63, 127.37, 114.25, 111.42, 107.96, 104.25, 77.37, 77.06, 76.74, 72.27, 55.30. Anal.Calcd for $C_{21}H_{19}NO_3$: C, 75.66; H, 5.74; N, 4.20. Found C, 76.36; H, 5.24; N, 4.18.

2.3. X-ray structures solution and refinement for the compounds

Single crystals X-ray crystallographic data were collected on a Bruker APEX 2 CCD diffractometer. The crystals were kept at 293(2) K during data collection. Using Olex2 (Dolomanov et al., 2009), the structures were solved with the SHELXT (Sheldrick, 2015) structure solution program using Intrinsic Phasing and refined with the SHELXL (Sheldrick, 2015) refinement package using least-squares minimization.

2.4. DNA interaction study

The FS-DNA stock solution was made in a Tris-HCl buffer with a pH of 7.4 and a concentration of 50 mM, then kept refrigerated for up to 72 h at 4 °C. The FS-DNA concentration was calculated in all experiments using the 260 nm absorption band and a molar absorption coefficient of 6600 L $mol^{-1}.cm^{-1}$ (Lakshmipraba et al., 2015). The relevant calculations were made based on this concentration. The purity of the stock FS-DNA solution was verified by the UV absorption rate (A260/A280 > 1.8) as a result of measurements taken at 260 and 280 nm to determine that FS-DNA did not contain protein impurity (Isika et al., 2020). Similarly, the ligand stock solutions were prepared in DMSO and then diluted with Tris-HCl buffer to the appropriate concentrations. The EtBr used in photoluminescence experiments was prepared in ethanol at a concentration of 3.0×10^{-3} mol. L^{-1} and used right away in the experiments. All experiments were performed in triplicate.

2.4.1. UV-visible spectroscopy studies

For the analyzing of the interaction between FS-DNA and compounds, absorption spectra were measured in the 200–700 nm wavelength range. Spectra obtained by adding specific amounts of FS-DNA by titration method were recorded for each ligand solution. All measurements were achieved in triplicate and the falcon tubes were gently shaken and incubated for 15 min before taking measurements of the corresponding spectrum of the mixture for each sample. The intrinsic binding constant K_b was obtained from the plot of [DNA]/($\varepsilon_a - \varepsilon_f$) versus [DNA] graphic, where [DNA] is the concentration of DNA. The absorption coefficient ε_a, ε_f, ε_b correspond to A_{obs}/Ligand], the extinction coefficient for the free compounds (5a-d), and the extinction coefficient of the ligand compounds in the bound form, respectively (Isika et al., 2020). The observed values were appointed to Eq. (1), with a slope equal to 1/(ε_b-ε_f) and the intercept equal to 1/[K_b(ε_b-ε_f)]. K_b was obtained from the ratio of the slope to the intercept (Isika et al., 2020).

$$[DNA]/(\varepsilon a - \varepsilon f) = [DNA]/(\varepsilon b - \varepsilon f) + 1/[Kb(\varepsilon b - \varepsilon f)] \quad (1)$$

2.4.2. Fluorescence spectroscopy studies

Fluorescence quenching experiments were conducted to investigate the interactions of DNA with the compounds. To investigate the binding properties of compounds with DNA, the FS-DNA solution was carefully mixed with the DNA:EtBr (10:1) concentration ratio of ethidium bromide (EtBr), prepared just before the experiment at 25 °C, 15 min before the measurements. The intercalation mode docking of EtBr molecules to the double helix structure of DNA causes a significant increase in EtBr fluorescence intensity. Then, various concentrations of ligand solutions were added to this mixture, allowing the final mixture to incubate for 15 min. The fluorescence spectra of the resulting final solutions were shown in the range of 500–700 nm with an excitation wavelength of 520 nm. Fluorescent quenching efficiency was evaluated according to the following equation (Stern–Volmer equation, Eq. (2)) (Isika et al., 2020).

$$I_0/I = K_{sv}[Q] + 1 \quad (2)$$

where I_0 and I are the intensities of the emission in the presence and absence of the quencher, K_{sv} is the quenching

binding constant, and [Q] is the concentration of the ligand (quencher). The slopes of the obtained plots of I_0/I versus [Q] were used to calculate the K_{sv} values (Isika et al., 2020).

2.5. Molecular docking studies

The synthesized compounds, 5a-d, were sketched in drawing BIOVIA Draw 2019 software, and their energies were minimized by Chem3D 20. The molecular docking analysis was conducted on the ligands against 1BNA as a model system by using the Autodock vina tool PyRx docking software (academic licensed version 0.9.8) (Dallakyan & Olson, 2015). The free DNA's high-resolution (1.90 Å) structure was downloaded from the PDB database (PDB code: 1BNA) (http://www.rcsb.org/pdb). In the next step, 1BNA was enclosed in a box with number of grid points in $x \times y \times z$ ($30 \times 25 \times 47$) directions, and docking was performed using a cubic box with $15 \times 21 \times 10$ dimensions. In this analysis, flexible-ligand:rigid-receptor docking was performed, and accurate docking conditions were selected. The docked complexes (5a-DNA, 5 b-DNA, 5c-DNA and 5d-DNA) were assessed on the lowest binding energy (kcal/mol) values. The graphical representations and related results of all the docking complexes were carried out and monitored using Discovery Studio 2020.

2.6. Preparation and cultivation of bacterial strains

The imine compounds were evaluated in vitro antibacterial and antifungal activity against the Staphylococcus aureus, Bacillus cereus as the gram (+); Escherichia coli and Salmonella typhimurium as the gram (-); and Candida albicans as the fungi. Antibiotics (Gentamicin and amikacin) were used as positive control groups. The susceptibility of a microorganism to antimicrobial agents and antibiotics was determined by assay plates incubated at 37 °C for 18–24 h for bacteria and 25 °C for three days for yeasts. In the antimicrobial activity studies, Malt Extract Agar (MEA) for the yeast strain and Müeller Hinton Agar (MHA) for bacteria were used as a stock medium. Bacteria standardized with 0.5 McFarland standard was inoculated to sterile prepared petri dishes and incubated for 1 h at 37 ± 1 °C (Balouiri et al., 2016). DMSO was used as control. Amikacin (AK: 30 mg) and Gentamicin (CN: 10 mg) were used as standards. The antimicrobial activity of the imine compounds was determined using Kirby-Bauer Disk Diffusion Method (Balouiri et al., 2016; C.L.S.I., 2012). The imine compounds (12.50 mg/mL) were dissolved in 10% DMSO and impregnated with disks at a concentration of 25 mL to discs made of blank sterile Whatman papers of 6 mm diameter. Prepared discs were placed on the cultivation of bacteria in the MHA. Discs were placed on planted cultures of bacteria in MHA and yeast strains in MEA. Discs were incubated at 37 ± 1 °C for 24 ± 2 h to determine inhibition zones (Bauer et al., 1966; Bradshaw, 1992; Lennette et al., 1974; Power & McCuen, 1988). The study was performed in three replicates and the mean values were given. The samples (**5a-d**) were 12.5 mg/mL, 1.25 mg/mL and 0.125 mg/mL dissolved in 10% DMSO to determine the minimum inhibitory concentration (MIC) against Gram positive (+), Gram negative (-) bacteria and yeast strains and the value was determined.

3. Results and discussion

3.1. Characterization of 5a-d

In the FT-IR spectra recorded for characterization of synthesized imine compounds, stretching peaks at 3443, 3431, 3401 and 3385 cm^{-1} are due to the phenolic hydroxyl group (ν_{OH}). The characteristic signals of imine groups (-C = N-) are the bands observed at 1623, 1619, 1628 and 1627 cm^{-1}. The absence of signals belonging to the carbonyl group in the starting salicylaldehyde derivatives in the spectrum of the result products also confirmed the formation of imine compounds.

The ^{1}H–^{13}C NMR spectra of the compounds were examined and the spectral data obtained were given in the experimental part and in the supplementary documents (Figures S1–S4). In the ^{1}H NMR spectra of synthesized compounds, especially the expected ortho and meta interactions in the salicylaldehyde ring can be seen very clearly. When the ^{1}H NMR spectra of the new imine compounds were examined, singlets for 5a-5d observed at 8.47, 8.36, 8.38 and 8.02 ppm respectively are the proton signals of the characteristic azomethine group (-CH = N-). Singlets observed at 5.62, 5.59, 5.70 and 5.62 ppm in the spectra of all ligands for 5a-5d are dibenzylic proton signals adjacent to the imine group, respectively. The methoxy groups in the structure of imine compounds resonated as singlet at 3.94, 3.80, 3.84, 3.81, 3.83 and 3.78 ppm, respectively. In the ^{13}C NMR spectra characteristic imine carbons resonated at 164.77, 164.22, 164.58 and 163.15 ppm, respectively. The other carbon atoms of 5a-d compounds resonated between 169.08 and 55.30 ppm. The ^{1}H–^{13}C NMR spectra of the ligands appear to be in complete agreement with the proposed structures.

Single crystals of compounds 5a and 5c were able to grow from the slow evaporation of the ethanol solutions of the compounds. X-ray crystallographic data are listed in Table 1. The structures of both compounds were solved in *monoclinic* unit cell $P2_1/n$ space group. The thermal ellipsoid plots of the compounds are shown in Figure 1. The C15-N1 bond distances in 5a and 5c are 1.2722(18) and 1.282(2) Å, respectively, showing characteristic C = N double bond distances. X-ray crystallographic data showed that both compounds are in phenol-imine tautomeric form in the crystalline state.

In the structures of the compounds, there is a phenol-imine (O2-H·····N1) intramolecular hydrogen bond. In the structure of 5a, two molecules are stacked *via* antiparallel π-π interactions between phenol rings (C16-C21) Figure 2. Crystal packing of 5a are further stabilized by C-H····· π and C-H·····O interactions. Compound SA36 contains a second hydroxy group (O3) located at the *meta* position with respect to the imine bond (C15 = N1). In the structure of 5c, molecules form dimers by hydrogen bonding between phenolic oxygen atoms (O3-H·····O2) under symmetry operation of 1 − x, −y, 1 − z. The dimers are further linked by weaker C10-H·····O1 interactions forming a supramolecular chain along the *c* axis. Packing plot of 5c is depicted in Figure 3.

Table 1. Crystal data information and structure refinement for 5a and 5c compounds.

Identification code	5a	5c
Empirical formula	$C_{22}H_{21}NO_3$	$C_{21}H_{19}NO_3$
Formula weight	347.40	333.37
Temperature/K	293(2)	293(2)
Crystal system	Monoclinic	Monoclinic
Space group	$P2_1/n$	$P2_1/n$
a/Å	12.4651(4)	13.6519(4)
b/Å	9.7941(3)	9.1288(3)
c/Å	15.8493(6)	14.4256(4)
α/°	90	90
β/°	108.862(4)	92.715(3)
γ/°	90	90
Volume/Å^3	1831.05(11)	1795.78(9)
Z	4	4
ρ_{calc}g/cm^3	1.260	1.233
μ/mm^{-1}	0.084	0.083
F(000)	736.0	704.0
Crystal size/mm^3	0.17 × 0.12 × 0.09	0.17 × 0.12 × 0.09
Reflections collected	6769	24334
Ind. Ref. [Rint]	4099 [R_{int} = 0.0191]	4421 [R_{int} = 0.0325]
Data/restraints/parameters	4099/0/239	4421/0/230
Goodness-of-fit on F^2	1.063	1.060
Final R indexes [I>=2σ (I)]	R_1 = 0.0461, wR_2 = 0.1104	R_1 = 0.0543, wR_2 = 0.1412
Final R indexes [all data]	R_1 = 0.0714, wR_2 = 0.1229	R_1 = 0.1015, wR_2 = 0.1652
CCDC	2049019	2049020

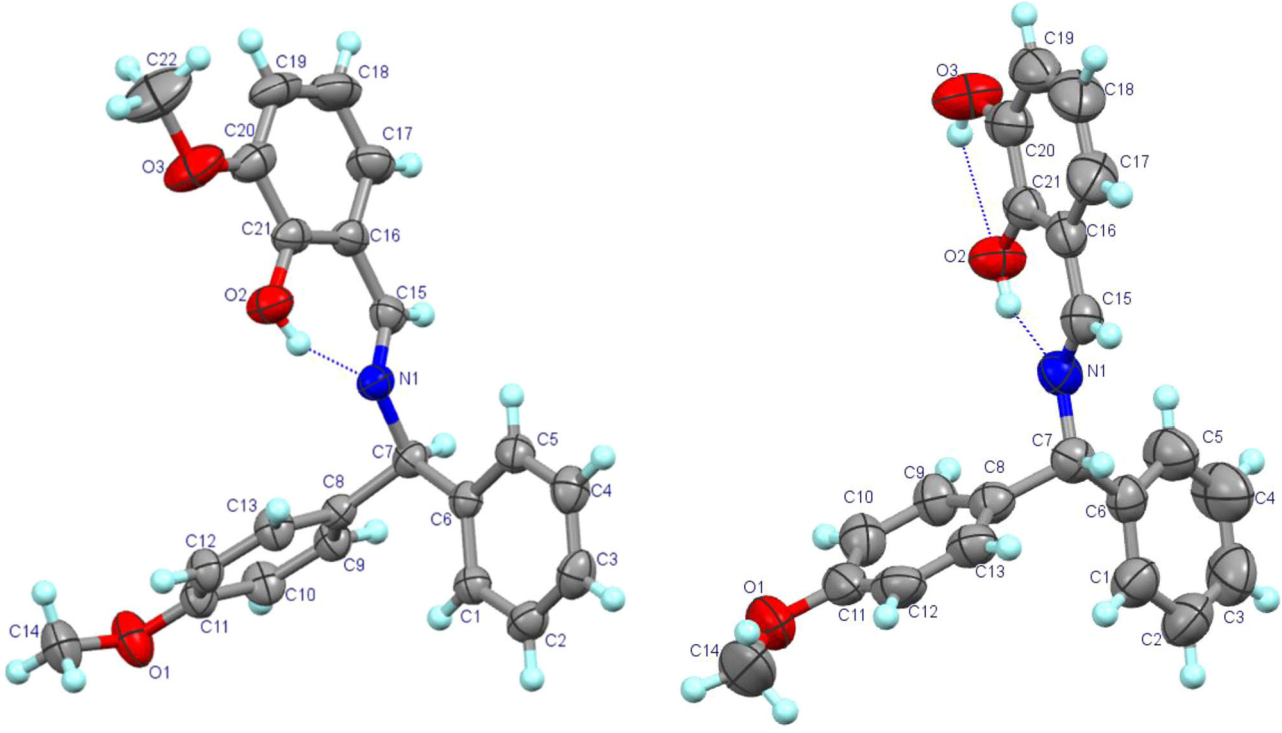

Figure 1. Thermal ellipsoid (50% probability) plots for compounds 5a and 5c.

3.2. Compound-DNA interaction study

3.2.1. Absorption spectroscopy studies

One of the most commonly used research techniques is electronic absorption spectroscopy, which is widely used to study DNA's interactions with small compounds. By a majority, the mechanism by which small molecules are bound to DNA by the intercalative binding mode has been enlightened, resulting in the hypochromic and bathochromic of the resultant absorption bands (Sirajuddin et al., 2013). Once electrostatic interaction occurs between DNA and compounds, a hyperchromic effect can be seen, with changes in the conformation of the DNA. However, in the case of the groove binding mode between DNA and compounds, the hypochromic effect can be recognized largely unchanged by the location of the absorption band; this can be attributed to the fact that the electronic states of the chromophore are superimposed on the DNA grooves of the complex with nitrogenous bases. (Shah et al., 2013; Xu et al., 2009).

To examine the interaction between FS-DNA and 5a-d compounds, UV-vis absorption spectra were measured in the presence and absence of various DNA concentrations. The UV-vis spectra of compounds 5a-d in the absence and

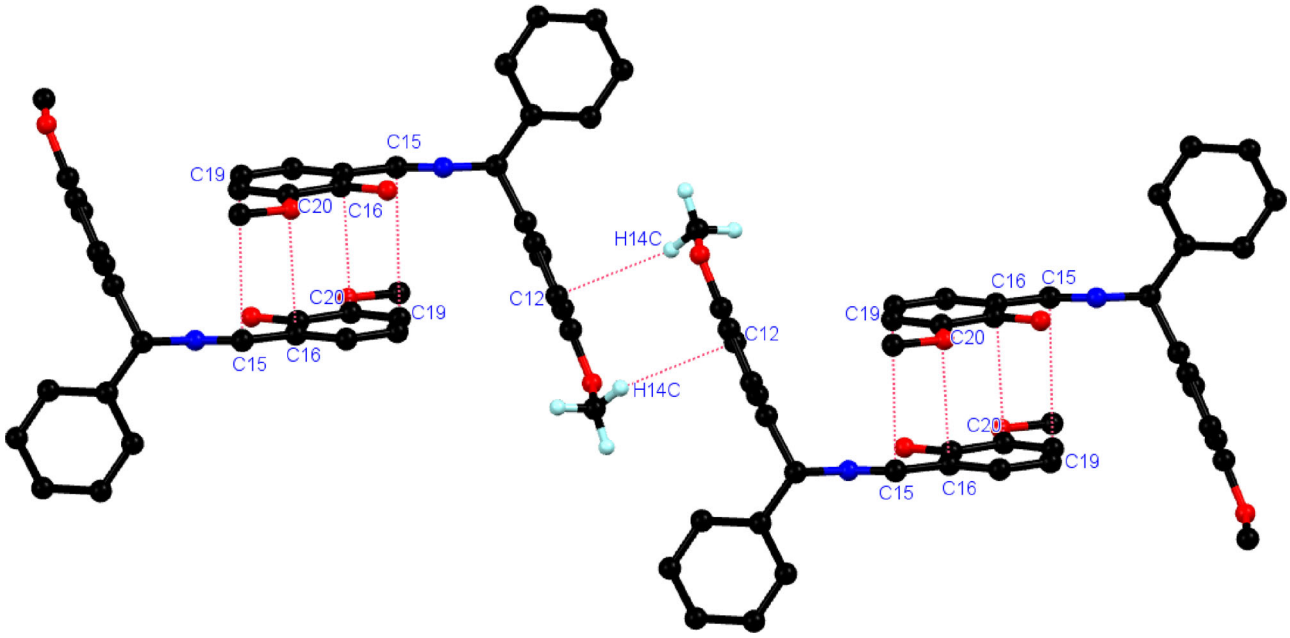

Figure 2. The π-π and CH·····π interactions in 5c.

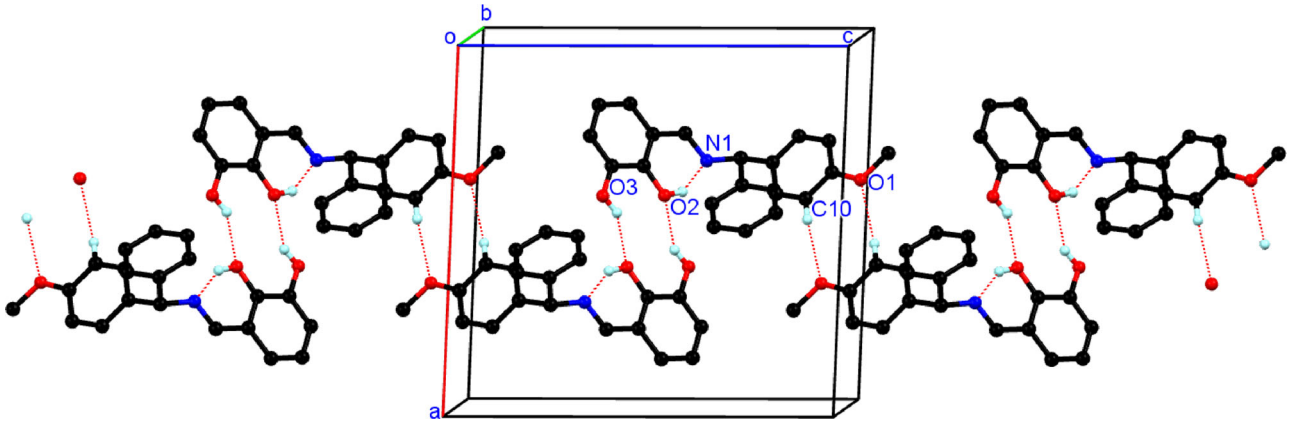

Figure 3. Packing diagram of 5c showing hydrogen bond interactions.

presence of FS-DNA are given in Figure 4. In the absence of DNA, 5a showed three different absorbance peaks at 245, 275, and 415 nm respectively. As the absorption in the 245 nm band increased with the addition of different DNA concentration, the absorption at 275 nm decreased and a partial red shift was observed. In compound 5 b, the absorption of the bands at 245, 300, 375 nm increased with the addition of DNA, while a slight blue shift was observed in the wavelength of the band at 300 nm. The maximum absorption peak at 265 nm seen in compound 5c started to become more pronounced with the gradual increase in DNA, and no shift was observed in the band seen at 360 nm. When the spectrum of the 5d compound is examined, the maximum absorption peaks at 240, 300 and 360 nm have increased steadily with the addition of DNA.

Based on changes in the absorption bands, the binding constant (K_b) for the ligand-DNA was calculated using the equation (Eq.1). The intrinsic binding constant (K_b) was found to be $3.56 \pm 0.3 \times 10^4\ M^{-1}$ for 5a, $2.18 \pm 0.2 \times 10^5\ M^{-1}$ for 5 b, $1.44 \pm 0.3 \times 10^5\ M^{-1}$ for 5c and $2.56 \pm 0.3 \times 10^4\ M^{-1}$ for 5d. When these values are compared with the classical intercalation agent Ethidium bromide, which is known to interact with DNA (although the EtBr-DNA (K_b=1,4 × 10^6) complex is significantly lower than binding) it can be said that it falls within the range of groove binding (J. H. Shi et al., 2015a) constant from binding modes when DNA interacts with a small molecule.

The absorption spectra of FS-DNA and its (5a-5d) DNA-Compound complexes formed by synthetic compounds are presented in Figure 5(a)–(d). When this figure is examined, it can be found that FS-DNA has a maximum absorption nearly at 260 nm, which is attributed to the chromophoric groups in the purine (adenine and guanine) and pyrimidine (cytosine and thymine) bases located within the sugar-phosphate backbone in the structure of DNA and responsible for electronic transitions (Dong et al., 2018; J.-H. H. Shi et al., 2018; J. H. Shi et al., 2015b). By gradually adding synthetic compounds at fixed concentrations (5a-5d) onto [DNA] at constant concentration, the UV absorbance of Fs-DNA showed a hypochromic effect with a negligible (around 1 nm) shift in wavelength. With this spectral change, it was concluded that

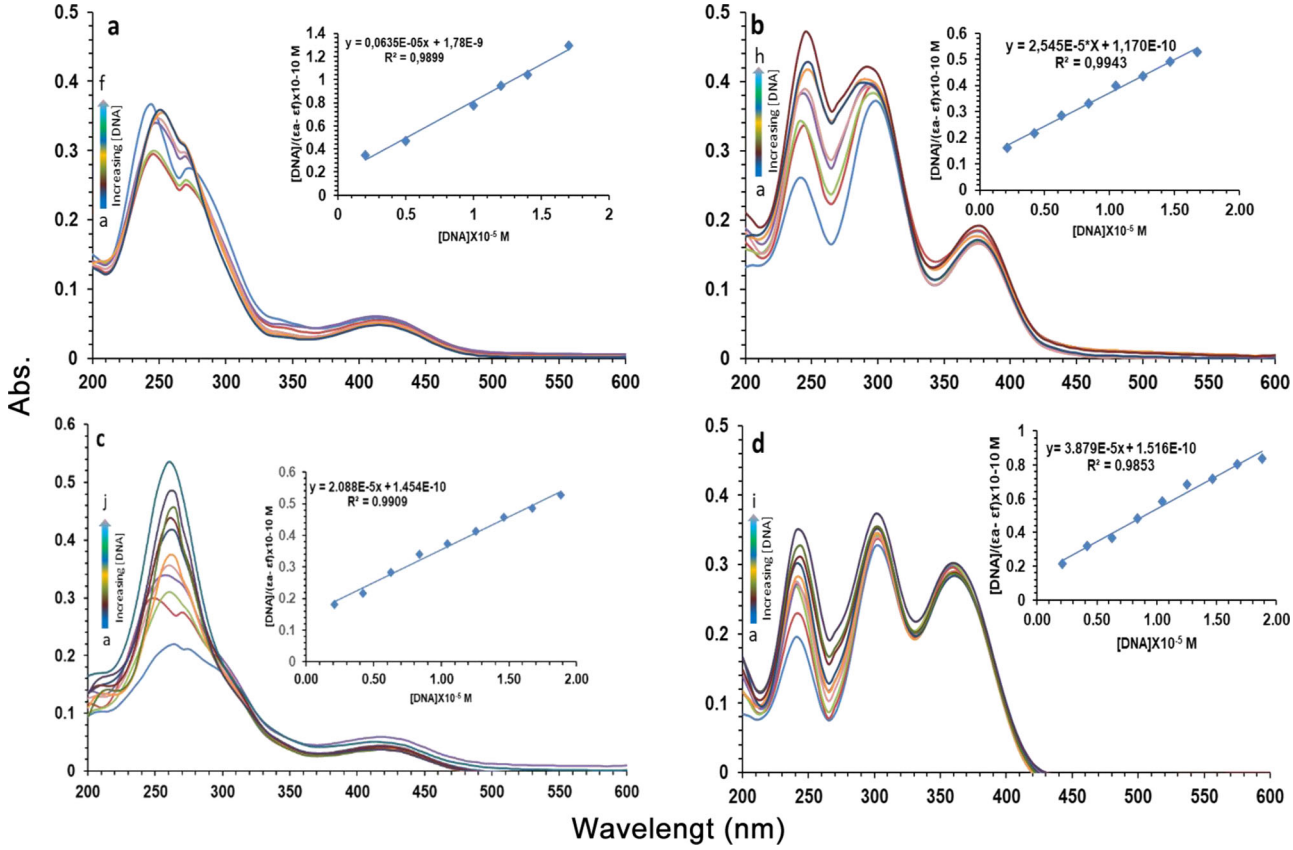

Figure 4. Absorption spectra of 20 μmol/L 5a (a), 20 μmol/L 5 b (b), 20 μmol/L 5c (c) and 20 μmol/L 5d (d) in the presence of FS-DNA at different concentrations (a: 0.0, b: 1.94, c:3.89 d: 5.84, e: 7.78, f: 9.73, g: 11.68, h: 13.63, i: 15.58, and j: 17.52 μmol/L in Tris-HCl buffer (0.1 mol/L, pH 7.4)). The inset showing the plot of [DNA/(εa-εf)] versus [DNA]. The corresponding solution of DNA was used as the reference solution.

the binding interaction of FS-DNA with synthetic compounds mainly might be an interaction in the groove binding mode, which is more acceptable (J.-H. H. Shi et al., 2018; J. H. Shi et al., 2018). To put it another way, when small molecules interact with DNA in the groove-binding mode, the position of the absorption band is almost unchanged, while the hypochromic effect can be observed, which can be explained by the overlapping of electronic positions of the chromophore with nitrogenous bases in the DNA-compound complex (J. H. Shi et al., 2018; J. H. Shi et al., 2015b).

3.2.2. Fluorescence quenching studies

Fluorescence quenching experiments were performed to further investigate the interaction mode of 5a-5d with DNA. EtBr, a strong intercalation agent known to interact with DNA, was chosen as a fluorescence indicator to research this interaction. Due to its robust location between adjacent DNA base pairs, EtBr has a poor fluorescence in the absence of DNA, but displays strong fluorescence at 597 nm when excited at 280 nm in the presence of DNA (intercalation). As a result, variations in this characteristic peak can be used to investigate the interaction of the compounds with FS-DNA. It has been determined in a previous study in the literature that by adding a second molecule, the increased fluorescence of DNA-EtBr can be quenched by a rivalry between EtBr and the second molecule to bind to DNA (Isika et al., 2020). While the addition of DNA solutions causes a large increase in the fluorescence intensity of EtBr, it also causes poor fluorescence emission in solution due to the transition of hydrogen into solution as a result of non-radiative degradation from the amino groups of EtBr (Jamshidvand et al., 2018). Hereby, these compounds can be used to replace EtBr by changing DNA conformation. As a consequence, the fluorescence is quenched as DNA-bound EtBr molecules are converted into their free forms in solution.

The fluorescence spectra of 5a-5d in the absence and presence of FS-DNA were shown in Figure 6. As 5a-5d compounds are gradually titrated into the EtBr-DNA complex, the maximum emission of the solution is reduced. This data has been validated by the interaction of the ligands with FS-DNA, which causes the formation of non-fluorescent complexes in both compounds and quenches the endogenous fluorescence. According to the Eq.2, the K_{SV} values of the compounds have been calculated to be $3.88 \pm 0.2 \times 10^3$, $4.41 \pm 0.2 \times 10^{3,}$ $5.26 \pm 0.3 \times 10^3$, $5.64 \pm 0.3 \times 10^3$ M^{-1} for 5a-5d respectively. K_{SV} values calculated from the Stern-Volmer equation are lower than the values of agents such as acridine orange, ethidium bromide, and methylene blue, which are well known to bind intercalation mode with DNA and find a wide place in the literature (Nafisi et al., 2007). Therefore, in the interaction of fluorescence DNA with competitive EtBr, it cannot be said for compounds to interact with DNA by intercalation and replace with EtBr (Sha et al., 2017). As can be seen from the fluorescence spectra, the decrease in the fluorescence intensity of EtBr-DNA with the

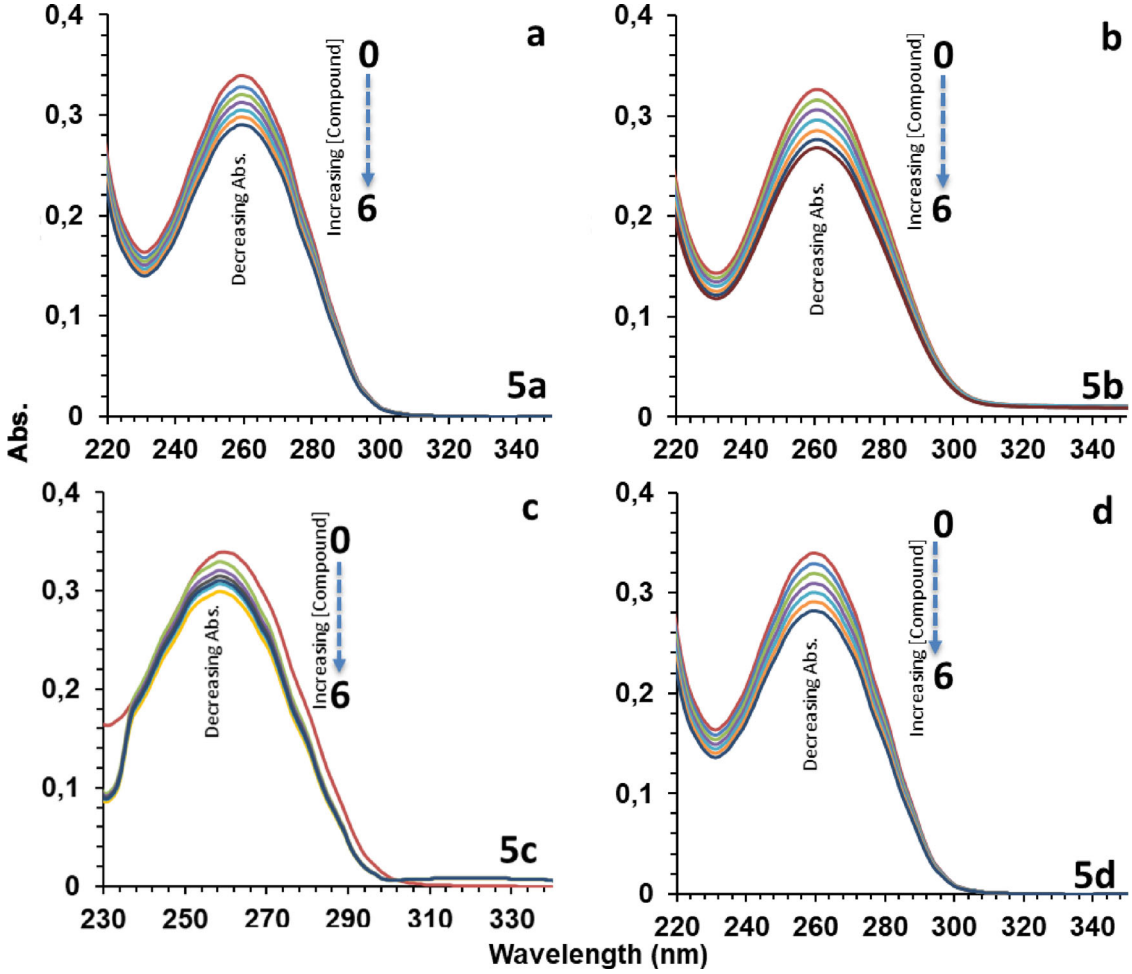

Figure 5. UV absorption spectra of FS-DNA (50 μmol/L) in the absence and presence of synthetic compounds (5a-5d) a:5a, b:5b, c:5c, d:5d. The concentration of synthetic compounds from 0 to 6 were 0: 0.0, 1: 1.94, 2:3.89 3: 5.84, 4: 7.78, 5: 9.73, 6: 11.68 μmol/L in Tris-HCl buffer (0.1 mol/L, pH 7.4)). The corresponding solutions of 5a-5d compounds was used as the reference solution.

addition of the compound is an indication that these compounds may be partially intercalated. However, this interaction is not very stable as in the EtBr-DNA system in line with the obtained K_{SV} values and fluorescence intensity of magnitude (Gan et al., 2020). The fact that the compounds have a partial intercalation mode is supported by molecular docking studies, which will be validated in the following sections.

3.3. Molecular docking studies

Studying the binding interaction mechanisms of biological macromolecules with small molecules has sparked a surge in molecular docking studies. Molecular docking is a valuable tool in rational drug design because it predicts the most stable structure and binding mode of the receptor-ligand complex structure, allowing interaction information to be identified appropriately and investigated during the production of new drugs. In critical stages of drug design and production, this method is often used as a virtual search tool (Isika et al., 2020). The preferred position of ligands on DNA may determine *via* molecular docking studies.

In molecular docking studies, docked compound conformations were analyzed in terms of energy, hydrogen bonding and interactions between DNA and molecules. According to the docking complex models with compounds and DNA, all compounds that bind to the major groove of DNA are also partially intercalated to the sugar-phosphate backbones. The binding energies were found to be −7.8, −7.7, −8.1 and −7.3 kcal/mol according to the best pose conformations for the 5a-5d, respectively. These scores relate to the set of minimum binding energy and maximum docking cluster. In addition, docking studies have shown that hydrogen and pi bond interactions are primarily prominent for the permanence of ligand-DNA structures. The optimal conformation poses of the ligand-DNA complexes based on their maximum binding energies for the four compounds are depicted in a 3D in Figure 7. These results are consistent with the spectroscopic results. When the 2D plot depiction of the interaction between DNA with 5a-d compounds is examined (Figure 8), for all compounds, DNA appears to have H bond interactions with both A and B chains of DNA. Considering the nucleotide bonding and molecular structures of 5a-5d it is seen that the conventional H and carbon H-bonds formed occur between all nucleotides of DNA and oxygen in the methoxy groups of the compounds. This suggests that the compounds have a

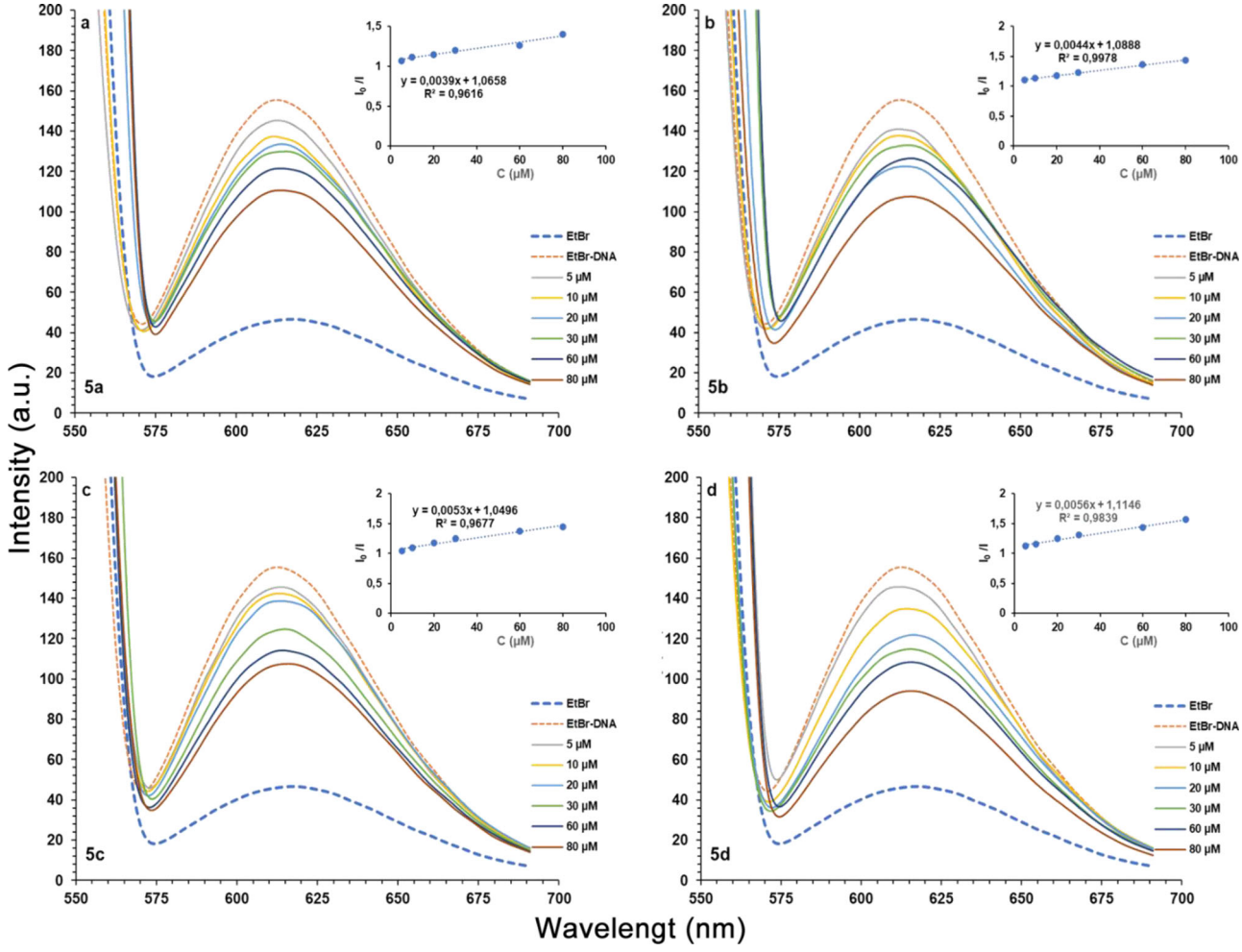

Figure 6. Quenching fluorescence spectra of FS-DNA bound to the EtBr system with the addition of ligands 20 μmol/L 5a (a), 20 μmol/L 5 b (b), 20 μmol/L 5c (c) and 20 μmol/L 5d (d) Inset: I_0/I versus [DNA](μM).

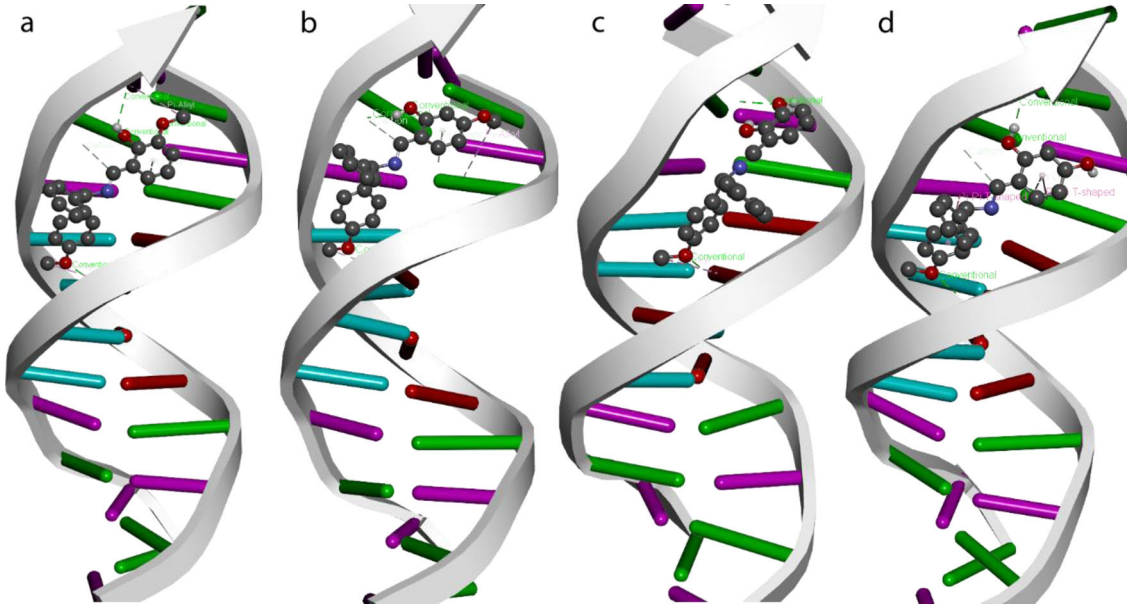

Figure 7. Molecular docked structure of 5a (a), 5 b (b), 5c (c) and 5d (d) complexed with DNA.

location between the opposite nucleotides in the DNA chains and bind in a partial intercalation mode, as indicated in fluorescence quenching studies. Besides, in all compounds except 5d, while the pi alkyl bond was observed in the oxygen and hydrogen atoms in the methoxy groups of the compounds, this situation was Pi-Pi T-shaped for 5d.

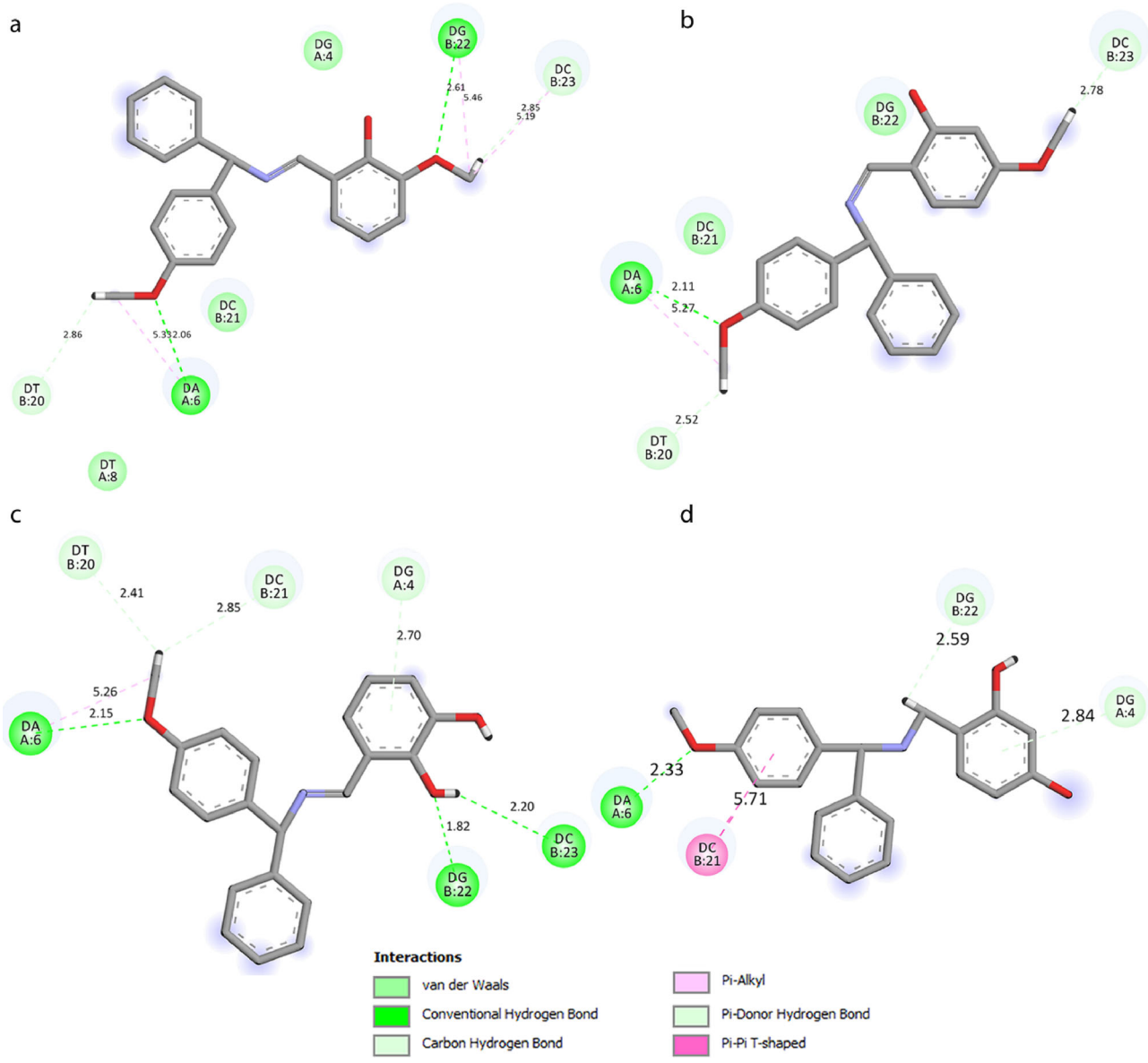

Figure 8. 2D plot of interaction between the 5a (a), 5 b (b), 5c (c) and 5d (d) with the dodecamer duplex sequence, d(CGCGAATTCGCG)$_2$ (PDB ID: 1BNA).

Table 2. Detailed residues with compound interactions-bonding types and distances of 5a, 5b, 5c and 5d with DNA complexes.

	Score (kcal/mol)	Interactions	Distance (A°)	**Bonding Types**	From	To
5A-DNA	−7.8	A:DA6:H3—:5 A:O21	2.06101	Conventional H Bond	A:DA6:H3	:5A:O21
		B:DG22:H3—:5 A:O7	2.60655	Conventional H Bond	B:DG22:H3	:5A:O7
		:5A:H7–B:DC23:O2	2.84868	Carbon H- Bond	:5A:H7	B:DC23:O2
		:5A:H15–B:DT20:O2	2.86155	Carbon H- Bond	:5A:H15	B:DT20:O2
		A:DA6–:5 A:C20	5.32569	Pi-Alkyl	A:DA6	:5A:C20
		B:DG22–:5 A:C8	5.46209	Pi-Alkyl	B:DG22	:5A:C8
5B-DNA	−7.7	A:DA6:H3–:5B:O21	2.11154	Conventional H Bond	A:DA6:H3	:5B:O21
		:5B:H8–B:DC23:O2	2.78114	Carbon H Bond	:5B:H8	B:DC23:O2
		:5B:H15–B:DT20:O2	2.52057	Carbon H Bond	:5B:H15	B:DT20:O2
		A:DA6–:5B:C22	5.26969	Pi-Alkyl	A:DA6	:5B:C22
5C-DNA	−8.1	:5C:H 14–B:DC23:O4′	2.20032	Conventional H Bond	:5C:H14	B:DC23:O4′
		A:DA6:H3–:5 C:O21	2.15337	Conventional H Bond	A:DA6:H3	:5C:O21
		B:DG22:H3–:5 C:O13	1.82145	Conventional H Bond	B:DG22:H3	:5C:O13
		:5C:H13–B:DT20:O2	2.41086	Carbon H- Bond	:5C:H13	B:DT20:O2
		:5C:H13–B:DC21:O4′	2.84588	Carbon H- Bond	:5C:H13	B:DC21:O4′
		A:DG4:H22–:5 C	2.69746	Pi-Donor H Bond	A:DG4:H22	:5C
		A:DA6–:5 C:C22	5.25542	Pi-Alkyl	A:DA6	:5C:C22
5D-DNA	−7.3	A:DA6:H3–:5D:O21	2.33093	Conventional H Bond	A:DA6:H3	:5D:O21
		:5D:H5–B:DG22:O4′	2.58835	Carbon H- Bond	:5D:H5	B:DG22:O4′
		A:DG4:H22–:5D	2.84181	Pi-Donor H Bond	A:DG4:H22	:5D
		:5D–B:DC21	5.71177	Pi-Pi T-shaped	:5D	B:DC21

Table 3. Antimicrobial activity values of the bacteria and fungi (mm)[a].

	Gram (−)		Gram (+)		Fungi
Compound	*Escherichia coli*	*Salmonella typhimurium*	*Staphylococcus aureus*	*Bacillus cereus*	*Candida albicans*
5a	8	8	10	10	–
5b	8	10	10	10	–
5c	8	10	10	8	–
5d	10	12	10	12	–
Amikacin	16	18	18	22	–
Gentamicin	12	18	18	16	–

–: Zone was not shown.
[a]Compounds (20 µL) in DMSO/H2O (1:9) were pipetted into the hollow agar at 12.5 mg/mL concentration.

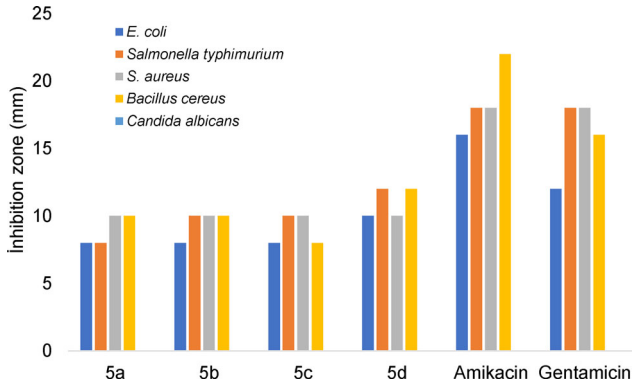

Figure 9. Antibacterial activity of the compounds showing inhibition zones in (mm).

In addition, there has been a significant change in the conformation of the molecules in their ability to bind along the major groove, and this conformational change is closely related to the structure of the DNA major groove. Besides, this situation can be evaluated as an important indicator of the formation of a complex structure between DNA and compounds. Data shows, bond types and bond lengths formed between nucleotides and ligands for compound-DNA complexes resulting from the docking process are summarized in Table 2.

3.4. Antimicrobial activity

In in vitro antimicrobial activity studies, we used *Escherichia coli* and *Salmonella typhimurium* as gram negative and *Staphylococcus aureus*, *Bacillus aureus* and *Bacillus cereus* as gram positive; *Candida albicans* as fungi. Amikacin and gentamicin antibiotics were used as positive control group. Antimicrobial activities of the ligands (5a-d) used in the study were investigated against Gram (+), Gram (-) bacteria strains and *Candida albicans* fungi by disk diffusion method. The results were compared with the standard antibiotics amikacin and gentamicin. The observed antimicrobial activities of the ligands are shown in Table 3. According to the findings, 5a ligand against *Staphylococcus aureus* and *Bacillus cereus* strains, 5b ligand against *Salmonella typhimurium*, *Staphylococcus aureus* and *Bacillus cereus* strains, 5d ligand against *Salmonella typhimurium* and *Bacillus cereus* strains showed moderate level of activity against *Salmonella typhimurius* and *Bacillus strains*. Antimicrobial activity of the complexes are shown in Figure 9 and summarized in Table 3.

4. Conclusion

New imino-methoxy derivatives have been successfully synthesized in this study. Fluorescence quenching and UV–Vis spectroscopy were used to investigate how these compounds bound to DNA. In addition, the molecular docking approach was used to examine the atomic specifics of these ligand-DNA interactions. The findings of the in-silico DNA-compound interaction studies indicate that compounds are groove binders, with hydrogen and pi bond interactions playing a key role in the ligand-DNA complexes stability. The current study demonstrates the mode of binding interaction, binding affinity, key ligand–FS-DNA interaction powers, and structure of the ligand–FS-DNA complex.

Acknowledgements

The authors are thankful to the Scientific Research Projects Unit of Kahramanmaraş Sütcü Imam University (Project code: BAP-2017/6-34 M), (Turkey). Furthermore, we would like to thank the Research Council of the Turkish Council of Higher Education (YÖK 100/2000) for awarding a postgraduate scholarship (to SO).

Disclosure statement

The authors declare no conflicts of interest.

ORCID

Sultan Onur http://orcid.org/0000-0003-4305-9638
Mustafa Çeşme http://orcid.org/0000-0002-2020-5965
Muhammet Köse http://orcid.org/0000-0002-4597-0858
Ferhan Tümer http://orcid.org/0000-0003-2222-2133

Credit authorship contribution statement

Sultan Onur: Investigation. Mustafa Çeşme: Data curation, Software, Writing—review & editing Investigation. Muhammet Köse: Data curation, Software, Writing—review & editing. Ferhan Tümer: Supervision, Project administration, Writing—Original draft.

References

Adımcılar, V., Çeşme, M., Şenel, P., Danış, İ., Ünal, D., & Gölcü, A. (2021). Comparative study of cytotoxic activities, DNA binding and molecular docking interactions of anticancer agent epirubicin and its novel copper complex. *Journal of Molecular Structure*, *1232*, 130072. https://doi.org/10.1016/j.molstruc.2021.130072

Allan, J. R., Gardner, A. R., McCloy, B., & Smith, W. E. (1992). Structural and thermal studies of the chloro complexes of cobalt, nickel and copper with 2,6-diaminopyridine and an assessment of their

suitability as anti-static additives for polyethylene. *Thermochimica Acta*, *208*(C), 125–131. https://doi.org/10.1016/0040-6031(92)80158-S

Ameen, D., & Snape, T. J. (2013). Chiral 1,1-diaryl compounds as important pharmacophores. In *MedChemComm* (Vol. 4, No. 6, pp. 893–907). The Royal Society of Chemistry. https://doi.org/10.1039/c3md00088e

Ashton, M. J., Ashford, A., Loveless, A. H., Riddell, D., Salmon, J., & Stevenson, G. V. (1984). Heterocyclic analogues of chlorcyclizine with potent hypolipidemic activity. *Journal of Medicinal Chemistry*, *27*(10), 1245–1253. https://doi.org/10.1021/jm00376a002

Balouiri, M., Sadiki, M., & Ibnsouda, S. K. (2016). Methods for in vitro evaluating antimicrobial activity: A review. *Journal of Pharmaceutical Analysis*, *6*(2), 71–79. https://doi.org/10.1016/j.jpha.2015.11.005

Bauer, A. W., Kirby, W. M., Sherris, J. C., & Turck, M. (1966). Antibiotic susceptibility testing by a standardized single disk method. *American Journal of Clinical Pathology*, *45*(4), 493–496. https://doi.org/10.1093/ajcp/45.4_ts.493

Bradshaw, L. J. (1992). Laboratory microbiology. *Acta Crystallographica Section A: Foundations and Advances* 4, 435.

C.L.S.I. (2012). Performance standards for antimicrobial disk susceptibility tests approved standard. In *CLSI document M02-A11* (Vol. 950, 7th ed.). Clinical and Laboratory Standards Institute.

Cardellicchio, C., Capozzi, M. A. M., & Naso, F. (2010). The Betti base: The awakening of a sleeping beauty. In *Tetrahedron asymmetry*. (Vol. 21, No. 5, pp. 507–517). Pergamon. https://doi.org/10.1016/j.tetasy.2010.03.020

Dahm, R. (2005). Friedrich Miescher and the discovery of DNA. *Developmental Biology*, *278*(2), 274–288. https://doi.org/10.1016/j.ydbio.2004.11.028

Dallakyan, S., & Olson, A. J. (2015). Small-molecule library screening by docking with PyRx. In J. E. Hempel, C. H. Williams, & C. C. Hong (Eds.), *Methods in molecular biology* (Vol. 1263, No. January, pp. 243–250). Springer. https://doi.org/10.1007/978-1-4939-2269-7_19

Di Santo, R., Tafi, A., Costi, R., Botta, M., Artico, M., Corelli, F., Forte, M., Caporuscio, F., Angiolella, L., & Palamara, A. T. (2005). Antifungal agents. 11. N-substituted derivatives of 1-[(aryl)(4-aryl-1H-pyrrol-3-yl)methyl]-1H-imidazole: Synthesis, anti-Candida activity, and QSAR studies. *Journal of Medicinal Chemistry*, *48*(16), 5140–5153. https://doi.org/10.1021/jm048997u

Dolomanov, O. V., Bourhis, L. J., Gildea, R. J., Howard, J. A. K., & Puschmann, H. (2009). OLEX2: A complete structure solution, refinement and analysis program. *Journal of Applied Crystallography*, *42*(2), 339–341. https://doi.org/10.1107/S0021889808042726

Dong, X.-M. M., Lou, Y.-Y. Y., Zhou, K.-L. L., & Shi, J.-H. H. (2018). Exploration of association of telmisartan with calf thymus DNA using a series of spectroscopic methodologies and theoretical calculation. *Journal of Molecular Liquids*, *266*, 1–9. https://doi.org/10.1016/j.molliq.2018.06.057

Gan, C., Huang, X., Zhan, J., Liu, X., Huang, Y., & Cui, J. (2020). Study on the interactions between B-norcholesteryl benzimidazole compounds with ct-DNA. *Spectrochimica Acta Part A: Molecular and Biomolecular Spectroscopy*, *227*, 117525. https://doi.org/10.1016/j.saa.2019.117525

Gemma, S., Campiani, G., Butini, S., Kukreja, G., Joshi, B. P., Persico, M., Catalanotti, B., Novellino, E., Fattorusso, E., Nacci, V., Savini, L., Taramelli, D., Basilico, N., Morace, G., Yardley, V., & Fattorusso, C. (2007). Design and synthesis of potent antimalarial agents based on clotrimazole scaffold: Exploring an innovative pharmacophore. *Journal of Medicinal Chemistry*, *50*(4), 595–598. https://doi.org/10.1021/jm061429p

Göppert-Mayer, M. (1931). Über Elementarakte mit zwei Quantensprüngen. *Annalen Der Physik*, *401*(3), 273–294. https://doi.org/10.1002/andp.19314010303

Güngör, Ö., Çeşme, M., Çınar, M. E., & Gölcü, A. (2019). The new metal-based compound from anticancer drug cytarabine: Spectral, electrochemical, DNA-binding, antiproliferative effect and in silico studies. *Journal of Molecular Structure*, *1193*, 532–543. https://doi.org/10.1016/j.molstruc.2019.05.014

Isika, D., Çeşme, M., Osonga, F. J., & Sadik, O. A. (2020). Novel quercetin and apigenin-acetamide derivatives: Design, synthesis, characterization, biological evaluation and molecular docking studies. *RSC Advances*, *10*(42), 25046–25058. https://doi.org/10.1039/D0RA04559D

Jamshidvand, A., Sahihi, M., Mirkhani, V., Moghadam, M., Mohammadpoor-Baltork, I., Tangestaninejad, S., Amiri Rudbari, H., Kargar, H., Keshavarzi, R., & Gharaghani, S. (2018). Studies on DNA binding properties of new Schiff base ligands using spectroscopic, electrochemical and computational methods: Influence of substitutions on DNA-binding. *Journal of Molecular Liquids*, *253*, 61–71. https://doi.org/10.1016/j.molliq.2018.01.029

Lakshmi, B., Shivananda, K. N., Prakash, G. A., Isloor, A. M., & Mahendra, K. N. (2012). Synthesis and characterization of schiff base metal complexes and reactivity studies with malemide epoxy resin. *Bulletin of the Korean Chemical Society*, *33*(2), 473–482. https://doi.org/10.5012/bkcs.2012.33.2.473

Lakshmipraba, J., Arunachalam, S., Solomon, R. V., Venuvanalingam, P., Riyasdeen, A., Dhivya, R., & Akbarsha, M. A. (2015). Surfactant-copper(II) Schiff base complexes: Synthesis, structural investigation, DNA interaction, docking studies, and cytotoxic activity. *Journal of Biomolecular Structure & Dynamics*, *33*(4), 877–891. https://doi.org/10.1080/07391102.2014.918523

Lennette, E. H., Spaulding, E. H., & Truant, J. P. (1974). *Manual of clinical microbiology* (7th ed., 970p). ASM Press. https://doi.org/10.4269/ajtmh.1971.20.3.tm0200030508a

McCord, J. M., & Fridovich, I. (1969). Superoxide dismutase. An enzymic function for erythrocuprein (hemocuprein). *Journal of Biological Chemistry*, *244*(22), 6049–6055. https://europepmc.org/article/med/5389100 https://doi.org/10.1016/S0021-9258(18)63504-5

Nafisi, S., Saboury, A. A., Keramat, N., Neault, J. F., & Tajmir-Riahi, H. A. (2007). Stability and structural features of DNA intercalation with ethidium bromide, acridine orange and methylene blue. *Journal of Molecular Structure*, *827*(1–3), 35–43. https://doi.org/10.1016/j.molstruc.2006.05.004

Onur, S., Köse, M., Koçer, F., & Tümer, F. (2020). Synthesis, characterization and antibacterial effect of diarylmethylamine-based imines. *Journal of Molecular Structure*, *1214*, 128150. https://doi.org/10.1016/j.molstruc.2020.128150

Plobeck, N., Delorme, D., Wei, Z. Y., Yang, H., Zhou, F., Schwarz, P., Gawell, L., Gagnon, H., Pelcman, B., Schmidt, R., Yue, S. Y., Walpole, C., Brown, W., Zhou, E., Labarre, M., Payza, K., St-Onge, S., Kamassah, A., Morin, P. E., … Roberts, E. (2000). New diarylmethylpiperazines as potent and selective nonpeptidic delta opioid receptor agonists with increased In vitro metabolic stability. *Journal of Medicinal Chemistry*, *43*(21), 3878–3894. https://doi.org/10.1021/jm000228x

Power, D. A., & McCuen, P. J. (1988). Manual of BBL products and laboratory procedures. In *Becton Dickinson Microbiology Systems* (6th ed., pp. 67–72). Becton, Dickinson and Company.

Riley, D. P., Lennon, P. J., Neumann, W. L., & Weiss, R. H. (1997). Toward the rational design of superoxide dismutase mimics: Mechanistic studies for the elucidation of substituent effects on the catalytic activity of macrocyclic manganese(II) complexes. *Journal of the American Chemical Society*, *119*(28), 6522–6528. https://doi.org/10.1021/ja964271e

Roy, D., & Panda, G. (2020). Benzhydryl amines: Synthesis and their biological perspective. *ACS Omega*, *5*(1), 19–30. https://doi.org/10.1021/acsomega.9b03090

Sha, Y., Chen, X., Niu, B., & Chen, Q. (2017). The interaction mode of groove binding between quercetin and calf thymus DNA based on spectrometry and simulation. *Chemistry & Biodiversity*, *14*(10), e1700133. https://doi.org/10.1002/cbdv.201700133

Shah, A., Nosheen, E., Munir, S., Badshah, A., Qureshi, R., Rehman, Z. U., Muhammad, N., & Hussain, H. (2013). Characterization and DNA binding studies of unexplored imidazolidines by electronic absorption spectroscopy and cyclic voltammetry. *Journal of Photochemistry and Photobiology B: Biology*, *120*, 90–97. https://doi.org/10.1016/j.jphotobiol.2012.12.015

Sheldrick, G. M. (2015). SHELXT - integrated space-group and crystal-structure determination. *Acta Crystallographica. Section A, Foundations and Advances*, *71*(Pt 1), 3–8. https://doi.org/10.1107/S2053273314026370

Shi, J. H., Chen, J., Wang, J., & Zhu, Y. Y. (2015a). Binding interaction between sorafenib and calf thymus DNA: Spectroscopic methodology, viscosity measurement and molecular docking. *Spectrochimica Acta*

Part A: Molecular and Biomolecular Spectroscopy, *136*(PB), 443–450. https://doi.org/10.1016/j.saa.2014.09.056

Shi, J. H., Liu, T. T., Jiang, M., Chen, J., & Wang, Q. (2015b). Characterization of interaction of calf thymus DNA with gefitinib: Spectroscopic methods and molecular docking. *Journal of Photochemistry and Photobiology B: Biology*, *147*, 47–55. https://doi.org/10.1016/j.jphotobiol.2015.03.005

Shi, J. H., Zhou, K. L., Lou, Y. Y., & Pan, D. Q. (2018). Multi-spectroscopic and molecular docking studies on the interaction of darunavir, a HIV protease inhibitor with calf thymus DNA. *Spectrochimica Acta Part A: Molecular and Biomolecular Spectroscopy*, *193*, 14–22. https://doi.org/10.1016/j.saa.2017.11.061

Shi, J.-H. H., Lou, Y.-Y. Y., Zhou, K.-L. L., & Pan, D.-Q. Q. (2018). Exploration of intermolecular interaction of calf thymus DNA with sulfosulfuron using multi-spectroscopic and molecular docking techniques. *Spectrochimica Acta Part A: Molecular and Biomolecular Spectroscopy*, *204*, 209–216. https://doi.org/10.1016/j.saa.2018.06.054

Sirajuddin, M., Ali, S., & Badshah, A. (2013). Drug-DNA interactions and their study by UV-Visible, fluorescence spectroscopies and cyclic voltametry. *Journal of Photochemistry and Photobiology B: Biology*, *124*(October 2015), 1–19. https://doi.org/10.1016/j.jphotobiol.2013.03.013

Soliman, A. A., & Linert, W. (2007). Structural features of ONS-donor salicylidene Schiff base complexes. In *Monatshefte fur Chemie* (Vol. 138, No. 3, pp. 175–189). Springer Wien. https://doi.org/10.1007/s00706-007-0585-6

Thomas, J. B., Herault, X. M., Rothman, R. B., Atkinson, R. N., Burgess, J. P., Mascarella, S. W., Dersch, C. M., Xu, H., Flippen-Anderson, J. L., George, C. F., & Carroll, F. I. (2001). Factors influencing agonist potency and selectivity for the opioid delta receptor are revealed in structure-activity relationship studies of the 4-[(N-substituted-4-piperidinyl)arylamino]-N,N-diethylbenzamides. *Journal of Medicinal Chemistry*, *44*(6), 972–987. https://doi.org/10.1021/jm000427g

Wang, B. L., Kou, S. B., Lin, Z. Y., & Shi, J. H. (2020). Investigation on the binding behavior between BSA and lenvatinib with the help of various spectroscopic and in silico methods. *Journal of Molecular Structure*, *1204*, 127521. https://doi.org/10.1016/j.molstruc.2019.127521

Xu, X., Wang, D., Sun, X., Zeng, S., Li, L., & Sun, D. (2009). Thermodynamic and spectrographic studies on the interactions of ct-DNA with 5-fluorouracil and tegafur. *Thermochimica Acta*, *493*(1–2), 30–36. https://doi.org/10.1016/j.tca.2009.03.017

Yang, L., Zhu, W., Fang, M., Zhang, Q., & Li, C. (2013). A new carbazole-based Schiff-base as fluorescent chemosensor for selective detection of Fe3+ and Cu2+. *Spectrochimica Acta Part A: Molecular and Biomolecular Spectroscopy*, *109*, 186–192. https://doi.org/10.1016/j.saa.2013.02.043